

2D fan-beam CT with independent source and detector rotation

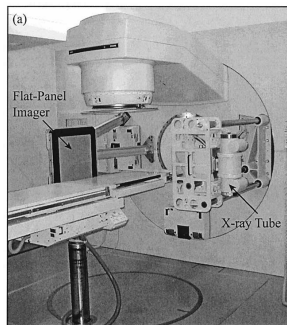
Simon Rit¹, Rolf Clackdoyle²

¹CREATIS / CLB / ESRF, University of Lyon, France

²LHC, Université Jean Monnet Saint Etienne, France

Image Guided Radiotherapy (IGRT)

- Imaging in the radiotherapy room
 - Fluoroscopy
 - Portal imaging
 - CT on rail
 - Ultrasound probe
 - ...
- Cone-beam CT since 10 years
 - Treatment guidance
 - Retrospective studies
 - Adaptive Radiotherapy

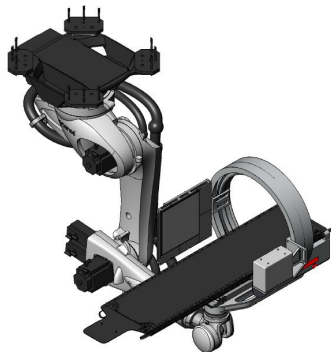


[Jaffray *et al.*, IJROBP, 2002]

New PAIR device (Salzburg)

Patient Alignment system with an integrated x-ray Imaging Ring

- Ceiling mounted robotic arm
- Independent rotation of the source and the flat panel
- Couch translation
- Source collimation with 4 motorized jaws
- Fast switching between energies
- $41 \times 41 \text{ cm}^2$ flat panel



medPhoton G.m.b.H
(courtesy of P. Steininger)

Installation: 1 prototype in Salzburg, 4 planned at MedAustron

Geometry in this presentation

[Gullberg *et al.*, IEEE TMI, 1986]

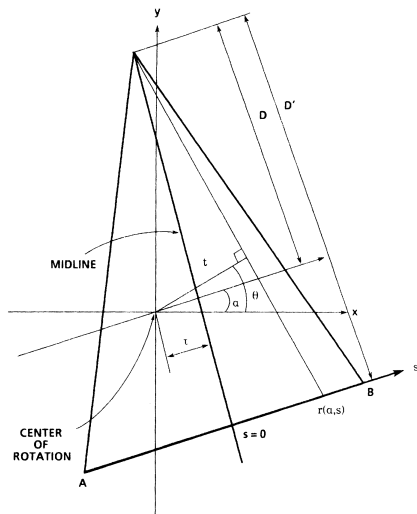


Fig. 2. Fan beam geometry with a displaced center-of-rotation for a flat detector.

Geometry in this presentation

[Gullberg *et al.*, IEEE TMI, 1986]

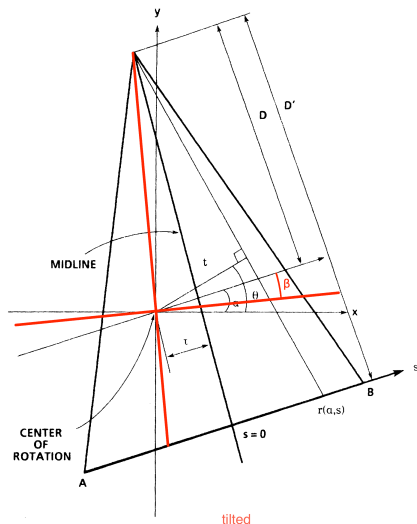
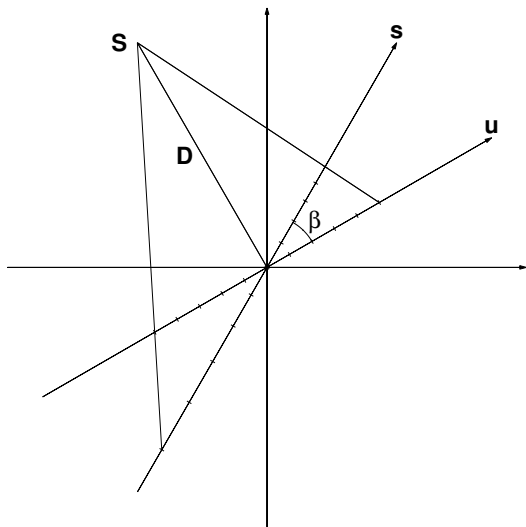


Fig. 2. Fan beam geometry with a displaced center of rotation for a flat detector.

Effect of tilt on sampling



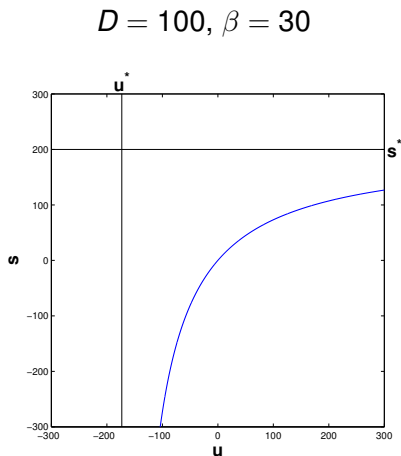
Effect of tilt on sampling

Relationship

$$s = \frac{uD}{D \cos \beta + u \sin \beta} \quad (1)$$

Limits

$$\begin{cases} u^* = \frac{-D}{\tan \beta} \\ s^* = \frac{D}{\sin \beta} \end{cases} \quad (2)$$



Effect of tilt on sampling

Derivative

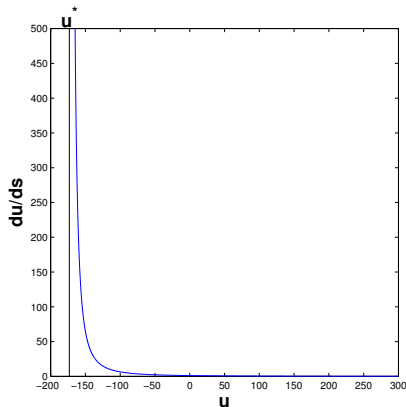
$$\frac{ds}{du} = \frac{D^2 \cos \beta}{(D \cos \beta + u \sin \beta)^2} \quad (3)$$

At origin,

$$\frac{ds}{du}(0) = \frac{1}{\cos \beta} \quad (4)$$

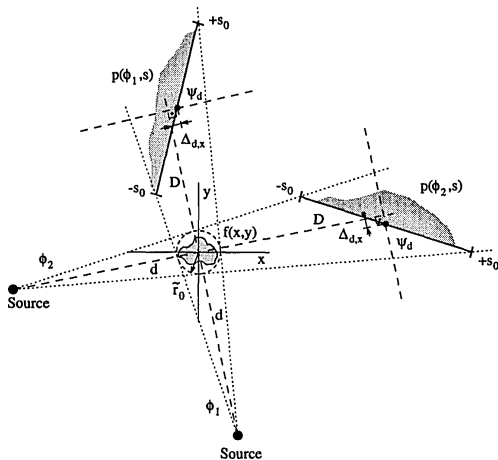
which would also be the constant sampling ratio in the parallel situation.

$$D = 100, \beta = 30$$



Potential use to increase spatial resolution

[Müller and Arce,
J Opt Soc Am A, 1994]



Inversion of the Radon transform

From parallel projections $p_p(\theta, t)$, the Fourier slice theorem leads to the inversion formula

$$f(r, \phi) = \int_0^{2\pi} \int_{-R}^R p_p(\theta, t) h[r \cos(\theta - \phi) - t] dt d\theta \quad (5)$$

with

$$h(t) = \int_{\mathbb{R}} \frac{|\mu|}{2} \exp^{2i\pi\mu t} d\mu. \quad (6)$$

Implementation: filtered backprojection algorithm.

Change of variable [Gullberg *et al.*, TMI, 1986]

Assuming a flat detector at the origin ($D=D'$), we have

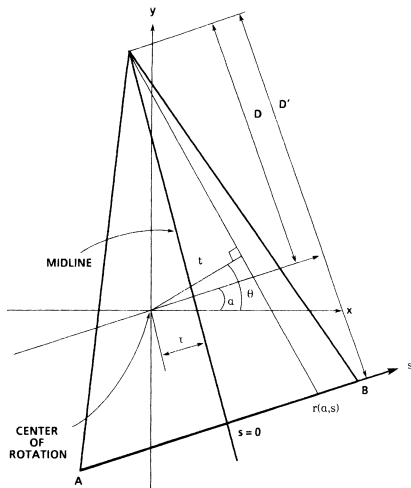
$$p_p(\theta, t) = p_f(\alpha, s) \quad (7)$$

for

$$\begin{cases} t = (s + \tau)Z \\ \theta = \alpha + \tan^{-1} \left(\frac{s}{D} \right) \end{cases} \quad (8)$$

with

$$Z = \frac{D}{\sqrt{s^2 + D^2}} \quad (9)$$



Assuming that D and τ are constant, the Jacobian matrix is

$$\frac{dt}{ds} = (D^2 - \tau s) \frac{Z^3}{D^2} \quad (10)$$

$$\frac{d\theta}{ds} = \frac{Z^2}{D} \quad (11)$$

$$\frac{dt}{d\alpha} = 0 \quad (12)$$

$$\frac{d\theta}{d\alpha} = 1 \quad (13)$$

so its determinant is

$$J = \left| \left(D^2 - \tau s \right) \frac{Z^3}{D^2} \right| \quad (14)$$

Change of variable [Gullberg *et al.*, TMI, 1986]

$$\begin{aligned} f(r, \phi) &= \int_0^{2\pi} \int_{-W}^W p_f(\alpha, s) h \left[r \cos(\alpha + \tan^{-1}(\frac{s}{D}) - \phi) - (s + \tau)Z \right] (D^2 - \tau s) \frac{Z^3}{D^2} ds d\alpha \\ &= \int_0^{2\pi} \int_{-W}^W p_f(\alpha, s) h [UZ(s' - s)] (D^2 - \tau s) \frac{Z^3}{D^2} ds d\alpha \end{aligned} \quad (15)$$

with

$$U = \frac{r \sin(\alpha - \phi) + D}{D} \quad (16)$$

$$s' = \frac{rD \cos(\alpha - \phi) - \tau D}{r \sin(\alpha - \phi) + D} \quad (17)$$

We can then use an essential property of the filter:

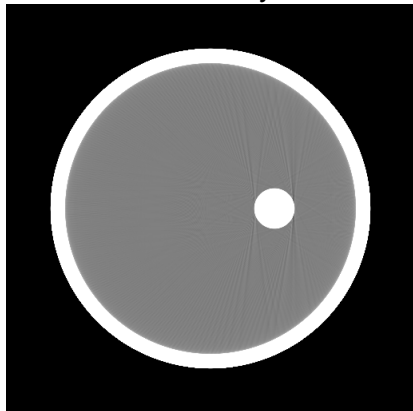
$$h(at) = \frac{1}{a^2} h(t) \quad (18)$$

to obtain

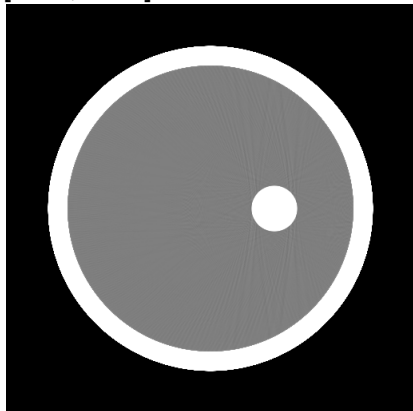
$$f(r, \phi) = \int_0^{2\pi} \frac{1}{U^2} \int_{-W}^W p_f(\alpha, s) \frac{D - \frac{\tau s}{D}}{\sqrt{s^2 + D^2}} h(s' - s) ds d\alpha \quad (19)$$

- $D = 630$ mm, $D' = 1100$ mm, $\tau = 1$ mm
- Projections
 - 1000
 - 768 samples
 - 0.2 mm spacing
- Reconstruction
 - 512×512 pixels
 - 0.125×0.125 mm² spacing

Gray level window: [-582, -482] HU.

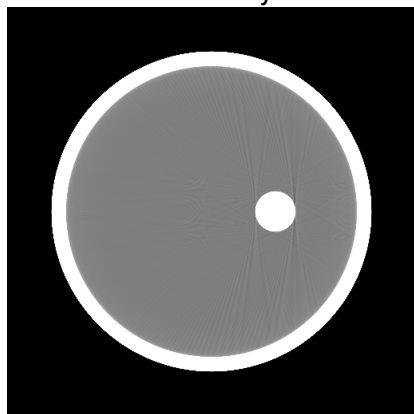


$\tau = 0$ mm

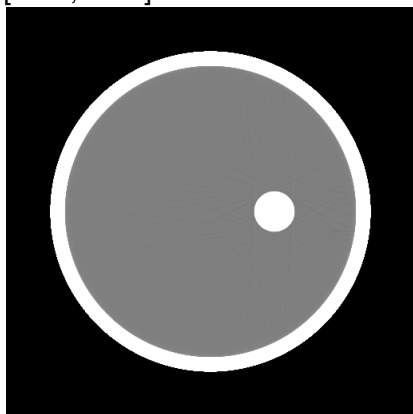


$\tau = 1$ mm, no correction

Gray level window: [-582, -482] HU.

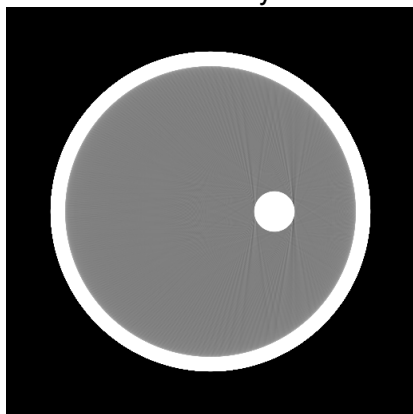


$\tau = 0$ mm

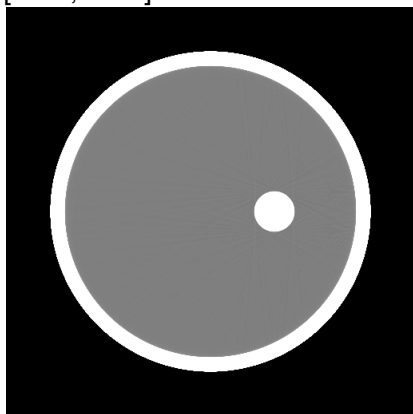


$\tau = 1$ mm, new algorithm

Gray level window: [-582, -482] HU.

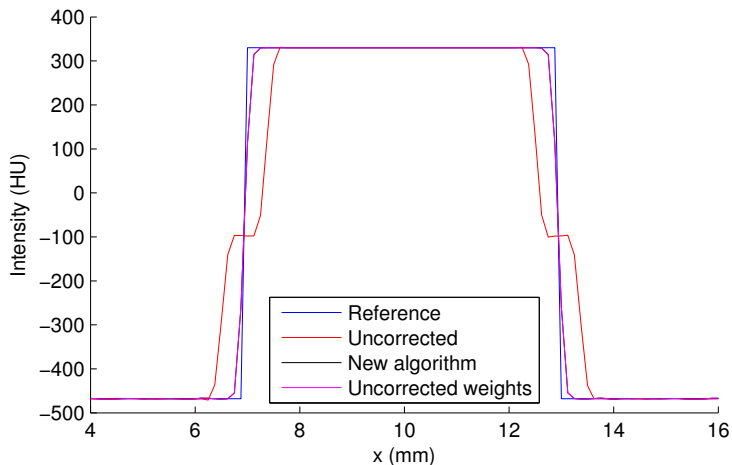


$\tau = 0$ mm



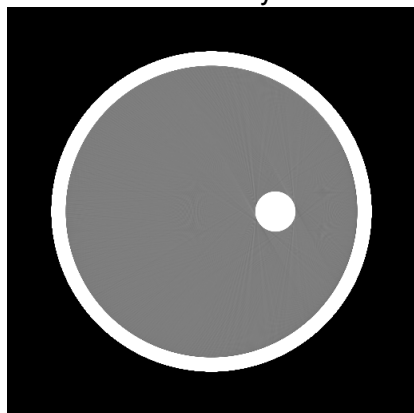
$\tau = 1$ mm, uncorrected weights

Experiments

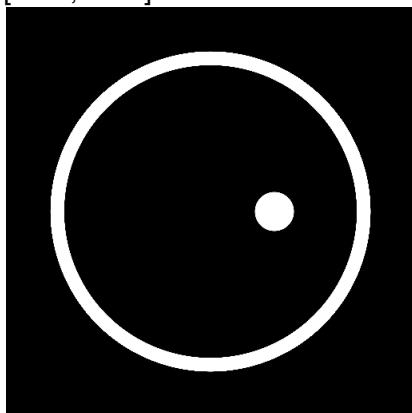


Experiments

Gray level window: [-582, -482] HU.

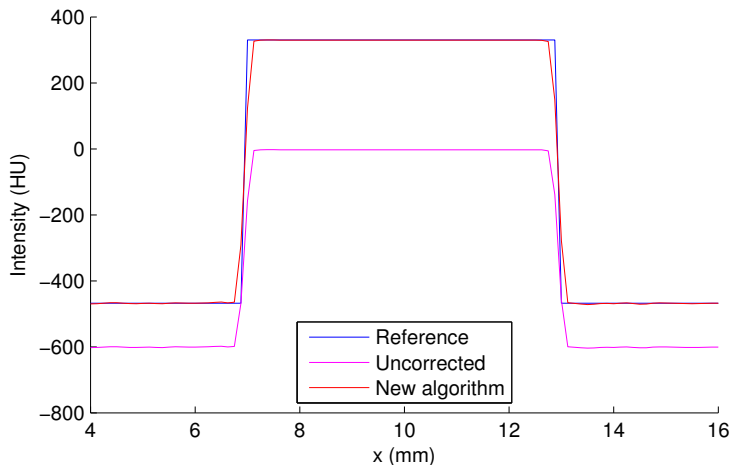


$\beta = 30^\circ$, new algorithm



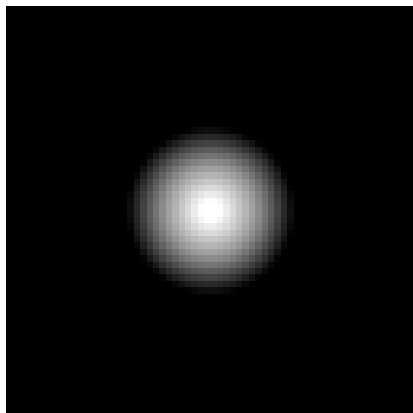
$\beta = 30^\circ$, uncorrected weights

Experiments



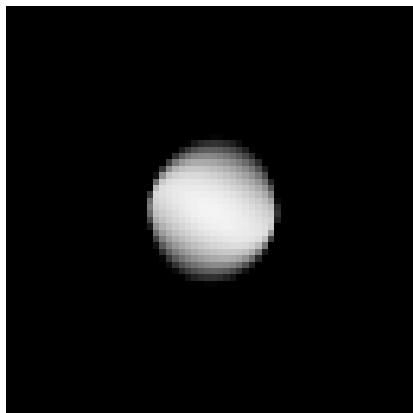
Point Spread Function

- $D = \tau = 1000$ mm, $\beta = 45^\circ$
- Ball at $(0, 0)$, radius 0.01 mm, density 1000 HU
- Projections
 - 1000 projections
 - 10 mm spacing
 - 1000 rays per pixel
- Reconstruction
 - Centered on $(0, 0)$
 - 64×64 pixels
 - $1 \times 1 \mu\text{m}^2$ spacing



Point Spread Function

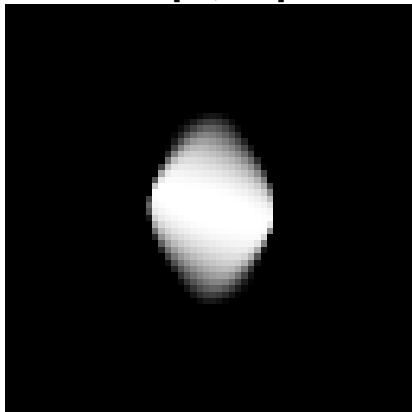
- $D = \tau = 1000$ mm, $\beta = 45^\circ$
- Ball at (800, 0), radius 0.01 mm, density 1000 HU
- Projections
 - 1000 projections
 - 10 mm spacing
 - 1000 rays per pixel
- Reconstruction
 - Centered on (800, 0)
 - 64×64 pixels
 - $1 \times 1 \mu\text{m}^2$ spacing



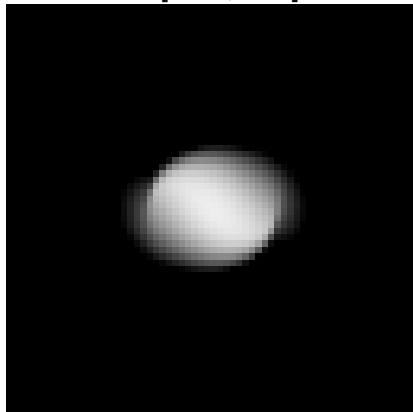
Point Spread Function

Short scan [Parker, Med Phys, 1982]

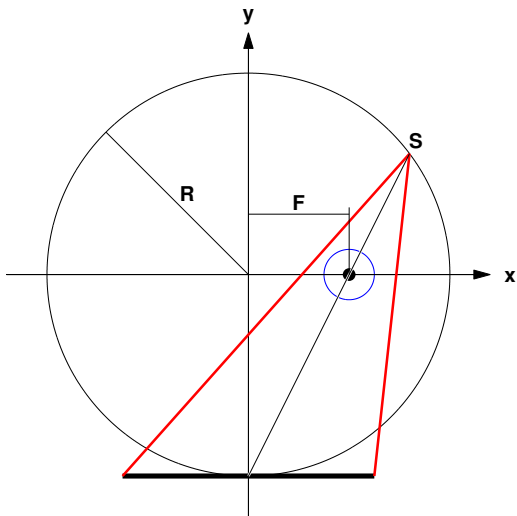
Arc $[50, 310]^\circ$



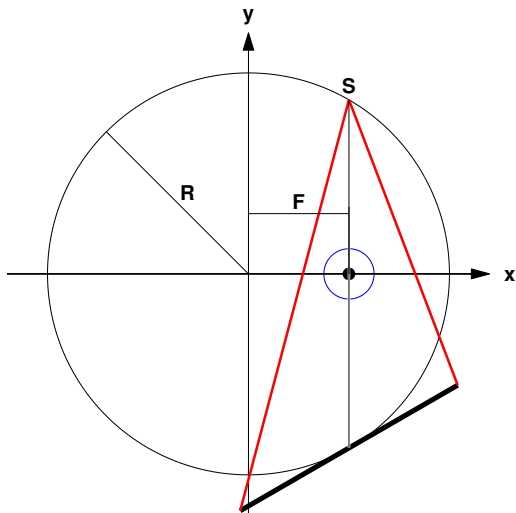
Arc $[-130, 130]^\circ$



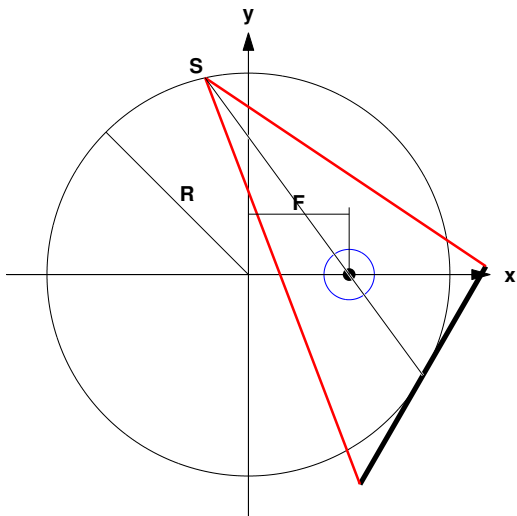
Independent source and detector rotation



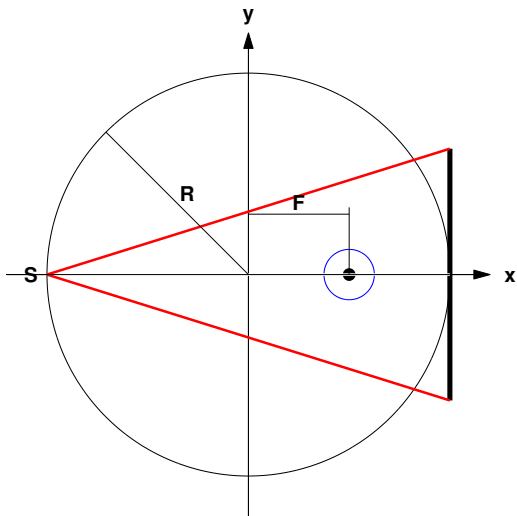
Independent source and detector rotation



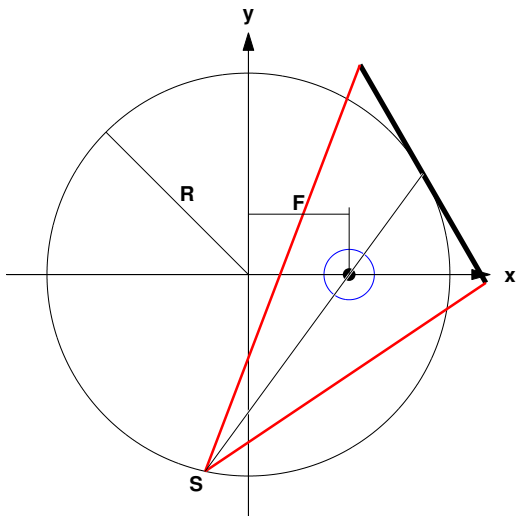
Independent source and detector rotation



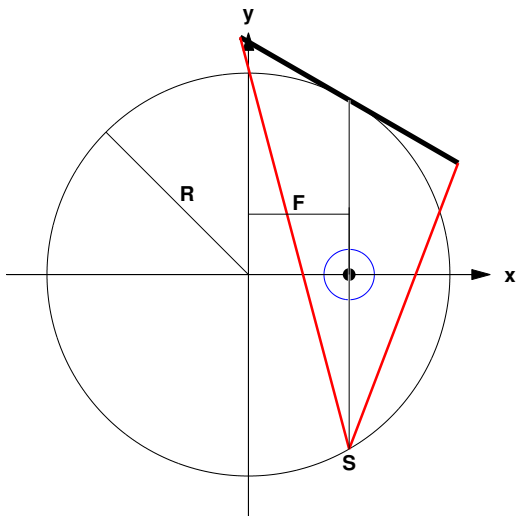
Independent source and detector rotation



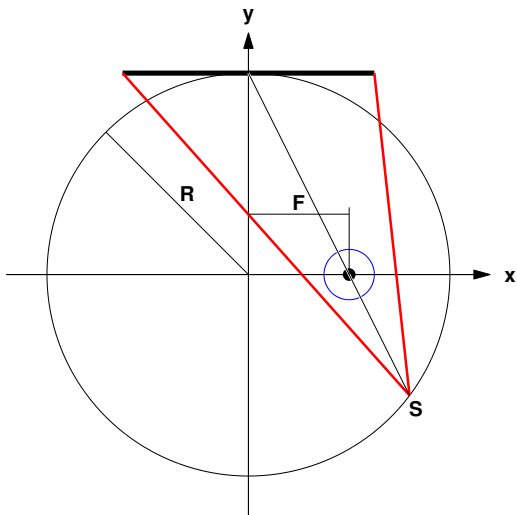
Independent source and detector rotation



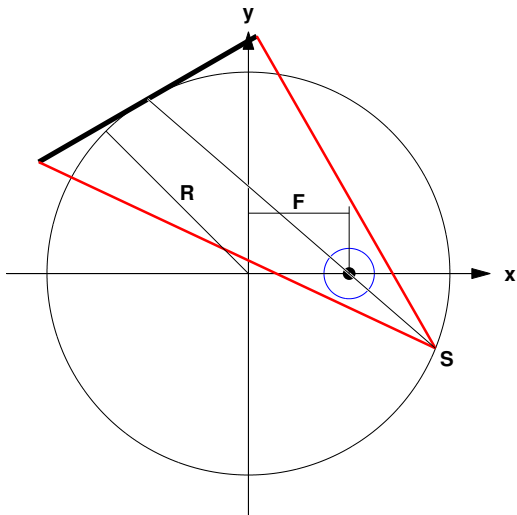
Independent source and detector rotation



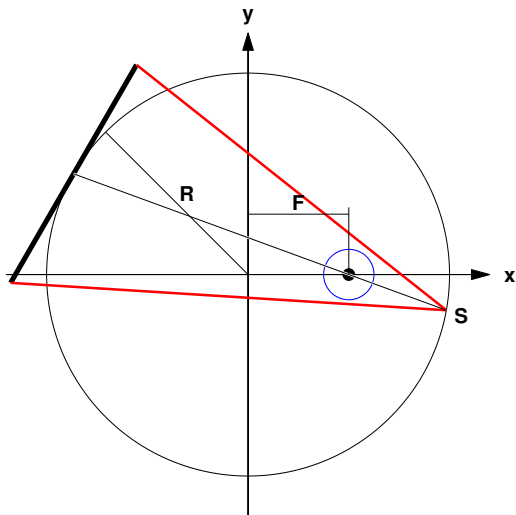
Independent source and detector rotation



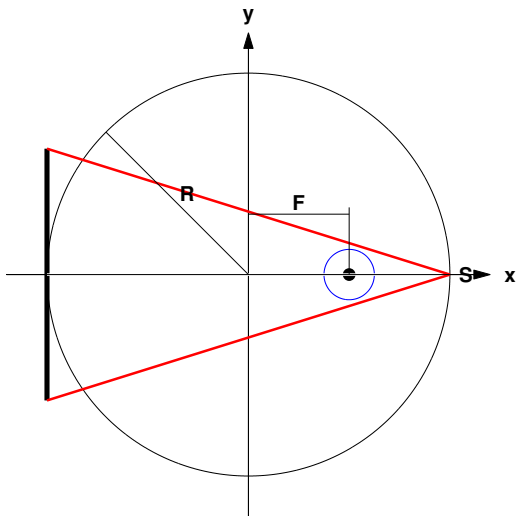
Independent source and detector rotation



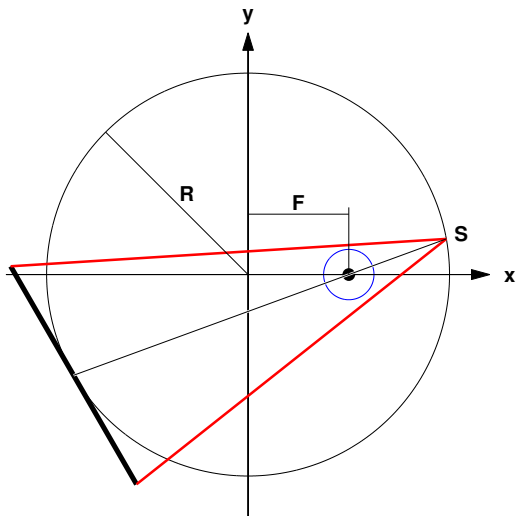
Independent source and detector rotation



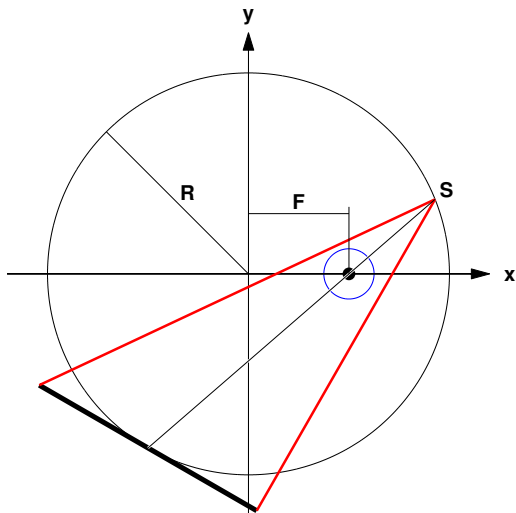
Independent source and detector rotation



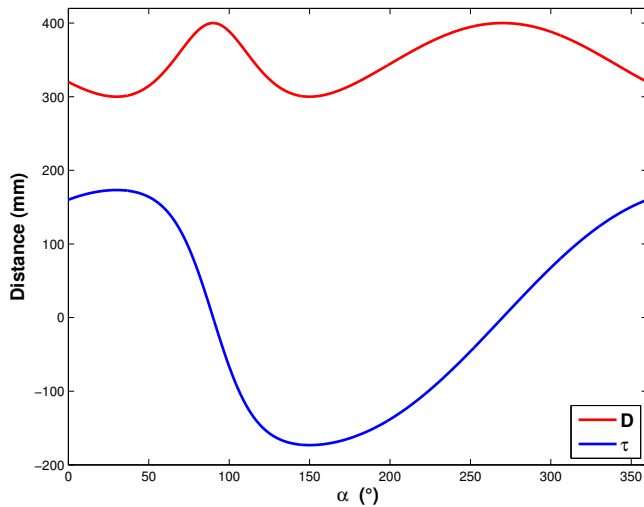
Independent source and detector rotation



Independent source and detector rotation



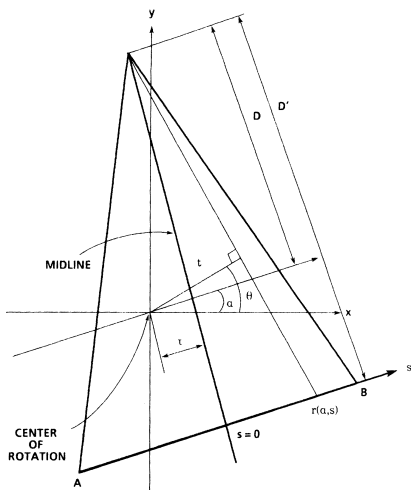
Independent source and detector rotation



τ depends on the gantry angle

$$\Rightarrow \tau : \alpha \rightarrow \tau(\alpha) \quad (20)$$

Note that the exact same derivation has been performed by [Concepcion *et al.*, IEEE TMI, 1992]



Change of variable [Crawford *et al.*, Med Phys, 1988]

Assuming D constant and τ constant, the Jacobian matrix is

$$\frac{dt}{ds} = (D^2 - \tau s) \frac{Z^3}{D^2} \quad (21)$$

$$\frac{d\theta}{ds} = \frac{Z^2}{D} \quad (22)$$

$$\frac{dt}{d\alpha} = Z \frac{d\tau}{d\alpha} \quad (23)$$

$$\frac{d\theta}{d\alpha} = 1 \quad (24)$$

so its determinant is

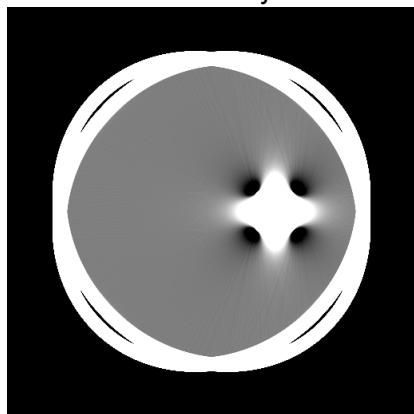
$$J = \left| \left(D^2 - \tau s - D \frac{d\tau}{d\alpha} \right) \frac{Z^3}{D^2} \right| \quad (25)$$

Inversion formula

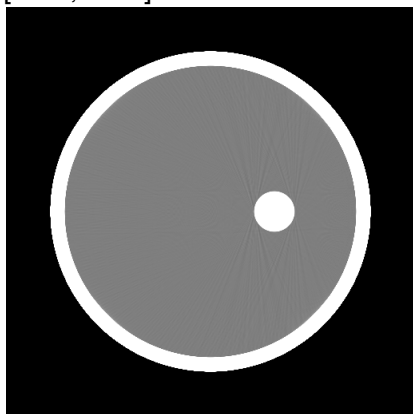
$$f(r, \phi) = \int_0^{2\pi} \frac{1}{U^2} \int_{-W}^W p_f(\alpha, s) \frac{D - \frac{\tau s}{D} - \frac{d\tau}{d\alpha}}{\sqrt{s^2 + D^2}} h(s' - s) ds d\alpha \quad (26)$$

In [Concepcion *et al.*, IEEE TMI, 1992], opposite sign for the new term. Mathematically wrong but experimentally correct (work in progress)...

Gray level window: [-582, -482] HU.



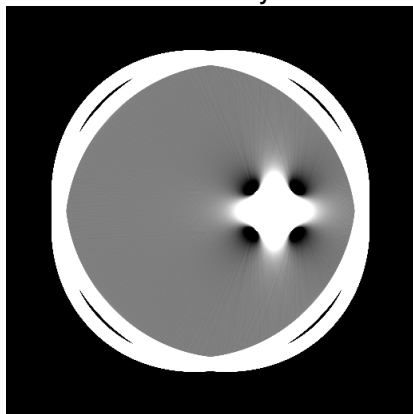
Assuming $\tau = 0$ mm



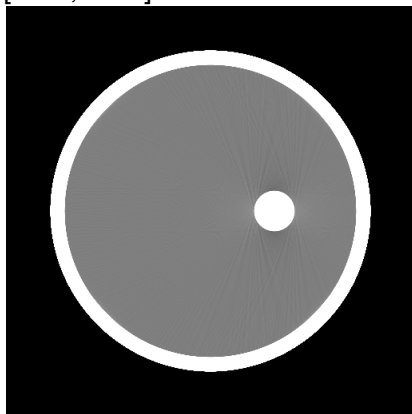
Actual $\tau(\alpha) = 3 \sin(2\alpha)$ mm

Experiments [Crawford *et al.*, Med Phys, 1988]

Gray level window: [-582, -482] HU.



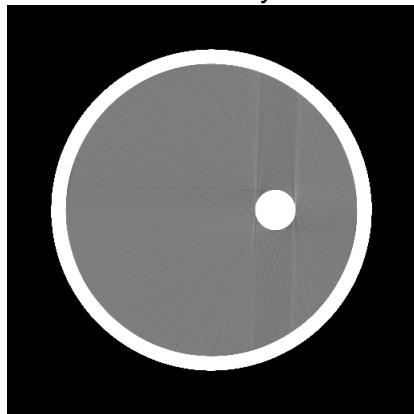
Assuming $\tau = 0$ mm



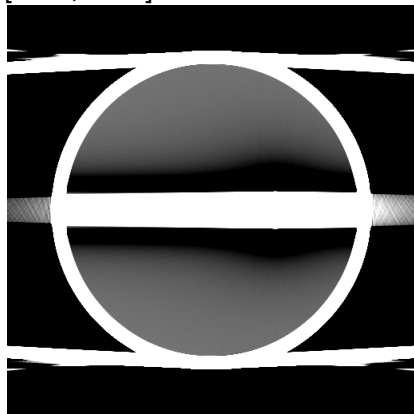
Assuming $\frac{d\tau}{d\alpha} = 0$ mm

Experiments

Gray level window: [-582, -482] HU.



Actual $\tau(\alpha) =$
 $630 \times \tan(30^\circ) \sin(2\alpha)$ mm

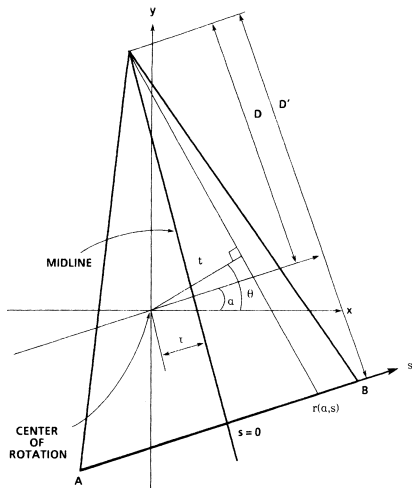


Assuming $\frac{d\tau}{d\alpha} = 0$ mm

Going further

D also depends on the gantry angle

$$\Rightarrow D : \alpha \rightarrow D(\alpha) \quad (27)$$



Change of variable

Assuming D constant and τ constant, the Jacobian matrix is

$$\frac{dt}{ds} = (D^2 - \tau s) \frac{Z^3}{D^2} \quad (28)$$

$$\frac{d\theta}{ds} = \frac{Z^2}{D} \quad (29)$$

$$\frac{dt}{d\alpha} = Z \frac{d\tau}{d\alpha} + (s + \tau) \frac{Z^3 s^2}{D^3} \frac{dD}{d\alpha} \quad (30)$$

$$\frac{d\theta}{d\alpha} = 1 - \frac{Z^2 s}{D^3} \frac{dD}{d\alpha} \quad (31)$$

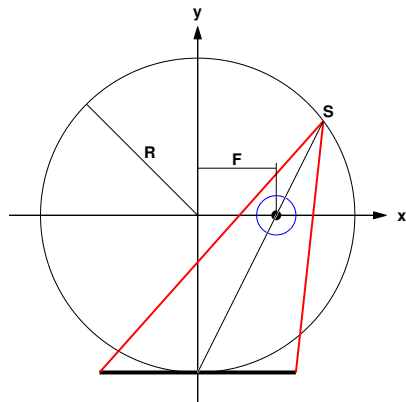
so its determinant is

$$J = \left| \left(D^2 - \tau s - D \frac{d\tau}{d\alpha} - s \frac{dD}{d\alpha} \right) \frac{Z^3}{D^2} \right| \quad (32)$$

Inversion formula

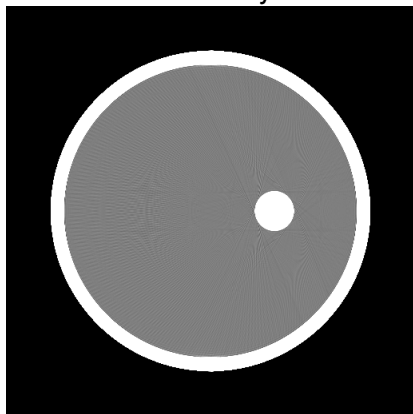
$$f(r, \phi) = \int_0^{2\pi} \frac{1}{U^2} \int_{-W}^W p_f(\alpha, s) \frac{D - \frac{\tau s}{D} - \frac{d\tau}{d\alpha} - \frac{s}{D} \frac{dD}{d\alpha}}{\sqrt{s^2 + D^2}} h(s' - s) ds d\alpha \quad (33)$$

Experiments

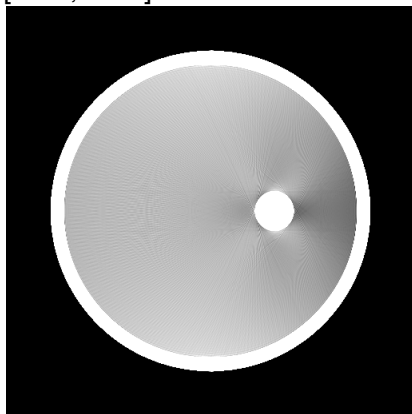


- $R = 200$ mm, $F = 100$ mm
- Projections
 - 2000
 - 1000 samples
 - 0.25 mm spacing
- Reconstruction
 - 512×512 pixels
 - 0.125 mm^2 spacing
 - Centered around $(F, 0)$

Gray level window: [-582, -482] HU.



New formula



Assuming $\frac{dD}{d\alpha} = 0$ mm

Conclusions

- Tilting an ideal detector improves CT resolution
- Inversion formula for any 2D derivable trajectory
- Requires the derivative of the parameters with respect to the gantry angle

Open questions

- What is the sensitivity to noise in geometric parameters?
- What is the optimal angular sampling?
- Will it really improve resolution when hardware considerations come into the picture?